

Finite Element Analysis of Circular Steel Concrete Composite Column

**Fatema-Tuz-Zahura¹, Razesh Kanti Sarkar², M.M.A. Anon³,
Farhan Faiaz Showvick⁴, S.M. Mostaq Ahmed Chowdhury⁵,
Md. Arif Arman Akash⁶**

¹Associate Professor, Department of Civil Engineering, Ahsanullah University of Science and Technology

²Lecturer, Department of Civil Engineering, Ahsanullah University of Science and Technology

^{3,4,5,6}Graduate Students, Department of Civil Engineering, Ahsanullah University of Science and Technology

Abstract

Because of its many benefits, concrete-filled tube (CFT) columns are composite structural elements that are frequently used in commercial and industrial structures. These columns have exceptional seismic resistance due to the combination of steel and concrete, which is demonstrated by their great strength, flexibility, and energy-absorbing capability. More specifically, in terms of aesthetic appeal and cost-effectiveness, circular hollow steel sections are preferable to open sections. This study examines the impacts of changing the diameter of the concrete core, the slenderness ratio of the hollow steel tube, and its thickness on CFT columns by a parametric analysis. The finite element analysis program ABAQUS was used to perform nonlinear analysis, and the outcomes demonstrated good agreement with experimental data. In comparison to the other two models, the model featuring a 160 mm diameter had the maximum displacement and load capacity for CFT columns with diameters of 140, 150, and 160 mm. The models with steel tube thicknesses of 6 mm, 4 mm, and 3 mm demonstrated the greatest displacement and load capacity, with the 6 mm thickness model leading the pack. The 600 mm model displayed the maximum displacement and load capacity for column heights of 600 mm, 500 mm, and 400 mm, whereas the shorter columns displayed lesser displacements and capacities. Furthermore, when the column height dropped, the discrepancy in the results grew. These results demonstrate how geometric features affect the functionality of CFT columns, highlighting how crucial it is to take these factors into account when designing and analyzing such structures.

Keywords: Concrete-filled tube, Steel tube, Displacement

1. Introduction

In modern building design, there is a growing emphasis on increasing floor space flexibility, which has led to a demand for columns with smaller cross sections. Enhancing the compressive strength of concrete allows for these smaller sections, using small amount of concrete with more usable space. However, reducing stirrup spacing to prevent brittle failure and achieve higher ductility in high-strength concrete can cause problems. This separation can create a natural distinction between the confined

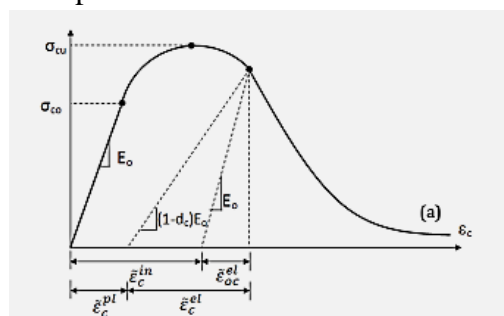
concrete core and the unconfined concrete cover, increasing the risk of premature spalling of the concrete cover (Claeson et al., 1998). One solution to this issue is the use of composite columns, specifically concrete-filled steel tubes (CFT), instead of traditional RCC columns. The use of composite columns has been increasing globally, driven by the development of high-strength concrete, which allows for more economical designs. In the thin steel casings, High-strength concrete minimizes the structural steel required while the high-strength concrete bears the majority of the compressive load. Research on composite columns started in the early 20th century and has come a long way since, despite the fact that composite columns made of steel and concrete were not often utilized between the end of World War II and the early 1970s.

(Johansson et al., 2002) investigated the mechanical performance of circular steel-concrete composite stub columns by testing 13 specimens under three different loading situations. The test results were supported by finite-element studies, which demonstrated that the way the load was applied had a significant impact on the mechanical performance of the columns. The behavior was unaffected by the strength of the bond when the steel and concrete components were loaded concurrently. While the confinement effects and, consequently, the mechanical properties of the columns were largely determined by the bond strength, the load was confined to the concrete part. Furthermore, (Huang et al., 2002) assessed 17 CFT column specimens with a higher diameter-to-thickness ratio. The impact of concrete strength and steel tube tensile strength on the behavior of composite columns was investigated by (Sakino et al., 2004). (Giakoumelis et al., 2004) tested fifteen times on circular CFT columns, examining the behavior of these columns in relation to the thickness of the steel tube plate, the connection between the steel tube and concrete, and the concrete confinement. Using the ABAQUS program, (Hu et al., 2003) created a 3-D nonlinear finite element model for CFT circular columns. Using a parametric analysis and trial and error, the numerical results were matched to produce the concrete confinement. To enhance the analytical outcomes of the ABAQUS program, a multi-linear stress-strain curve for the steel tube was employed, along with a modeling of the interface between the concrete and steel tube (Ellobody et al., 2006). The test findings have been compared to the accuracy of these analytical procedures. However, up until now, there hasn't been a clear connection established between the filled concrete, the steel tube's strength, and the diameter-to-thickness ratio of the concrete confinement. (Shibata et al., 2006) recently carried out a 3-D FEM simulation for the fracture behavior of CFT in axial compression. The experimental elements of composite steel-concrete columns with steel-encased profiles are described by (Campian et al., 2015). The columns constructed with high strength concrete performed better overall, particularly in terms of resistance, according to the data. It is still necessary to do additional experimental and numerical study because the high strength concrete fractures easily. According to (Liang et al., 2009) the steel tube in a circular concrete-filled steel tubular (CFST) short column creates a confinement effect that significantly increases the strength and ductility of the concrete core. Accurate models for constrained concrete are necessary for reliable prediction for circular CFST columns utilizing nonlinear analysis techniques. They provide precise constitutive models in their work for concrete with normal and high strengths that is contained by circular steel tubes of either type. In order to predict the nonlinear inflexible behavior of circular CFST short columns with axial loading, they constructed a general fiber element model and comprised these proposed constitutive models of limited concrete into it. The generated generic fiber element model is validated by the comparison of computed results with available experimental data. The correctness of various confining pressure models and the impact of steel yield strengths, concrete compressive strengths, and tube

diameter-to-thickness ratio on the basic behavior of circular CFST columns are investigated through extensive parametric investigations. For circular CFST columns, a new design formula that takes into consideration the impacts of concrete confinement are also suggested. It is shown that the design formula and generic fiber element model can be used to design normal and high-strength circular CFST columns, and that they can forecast the final strength and behavior of axially loaded circular CFST columns with sufficient accuracy. The tangent modulus approach provided cautious predictions for columns with L/D ratios less than 11 but good predictions for columns with L/D ratios larger than 11. It was found that the circular CFST short columns' strength was enhanced by the confinement effect. Shapes and the D/t ratio's impact on the behavior of CFST columns under axial force were investigated by (Tomii et al., 1977). Their research revealed that the strain hardening properties of the concrete confinement effect were seen in various octagonal and circular cross sections. Because of plate bending, square tubes provided minimal restriction to the concrete core. (Selah et al.,2021) investigated the experimental behavior of axially loaded short columns of CFST with D/t values ranging from 17 to 50. According to test results, compared to square or rectangular CFST columns, circular ones provided greater post-yield axial ductility. In order to investigate the effects of tube form, steel yield strengths, diameter-to-thickness ratio, and concrete strengths on the behavior of axially loaded CFST columns, (Sakino et al., 2004) evaluated 114 CFST columns. The design techniques for CFST columns were developed using the test results. (Giakoumelis et al.,2004) conducted experiments to examine how the strength of the bond between the concrete and steel tube, concrete confinement, and steel tube thickness affected, how circular CFST columns respond to an axial load. Their results demonstrated that the strength of the concrete has a major impact on the bonding strength between the steel tube and the concrete core. (Zeghiche et al., 2005) tested 27 CFTs. Slenderness, eccentricity, and single and double curvature were the test parameters. When the outcomes were compared to the EC4 guidelines, the twofold curvature resulted in the dangerous side. They recommended doing additional numerical and experimental research to verify the accuracy of Eurocode 4's buckling design techniques for high-strength concrete with single and double curvatures. Additionally, they said that the concrete's core strength declines with length of column and is only effective for shorter columns. One of the characteristics that can enhance ductile behavior was not varied in their tests: the D/t ratio. The consequences of altering the diameter of the concrete core, the slenderness ratio of the hollow steel tube, and its thickness were the main topics of this parametric study of CFT columns. In this study investigate that the forces with displacement for different diameter, length and thickness for CFT column.

2. Methodology

This study proposes an elastic-plastic-damage model. Scalar damage variables are introduced in order to describe the constitutive behavior of concrete. The CDP in Figure 1 can be used to describe the concrete's compressive and tensile response.



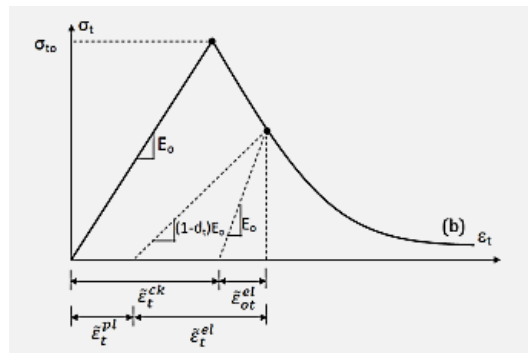


Figure 1: The ABAQUS User Manual (2008) describes the behavior of concrete under axial compressive (a) tension (b) strength.

As shown in Fig. 1, the specimen of unpacked concrete shows weakened response due to degraded elastic stiffness. Damage factors, d_t and d_c , which range from zero (undamaged) to one (complete strength loss), characterize this degradation, which can be seen on the strain-softening branch of the stress-strain curve (Abaqus User Manual, 2008). The stress-strain relation in the model is defined as in Eq. (3.1) and Eq. (3.2) (Tomasz Jankowiak et al., 2005)

$$\sigma_t = (1 - d_t) \cdot E_0 \cdot (\epsilon_t - \epsilon_t^{-pl}), \quad (3.1)$$

$$\sigma_c = (1 - d_c) \cdot E_0 \cdot (\epsilon_c - \epsilon_c^{-pl}). \quad (3.2)$$

Mesh sensitivity, caused by uneven cracking due to insufficient reinforcement, can be addressed using the fracture energy approach of Hillerborg, as opposed to the stress-strain relationship after failure. According to Fig. 2 of the Abaqus User Manual (2008), this method needs the specification of post-failure stress versus cracking displacement and treats the energy required to open a unit area of crack as a material attribute.

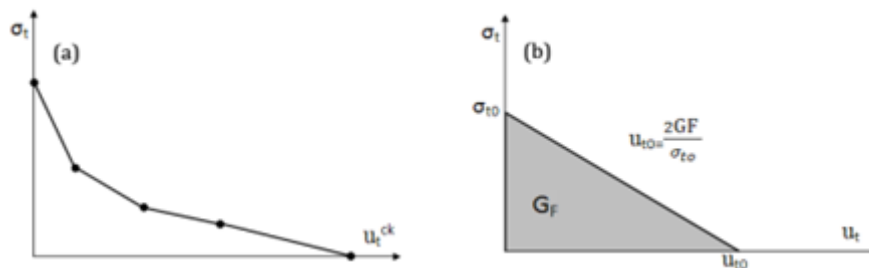


Figure 2: Post failure stress-strain relation with fracture energy approach (Abaqus User Manual, 2008)

The yield (or failure) surface size is determined by the effective cohesion stresses (Fig. 3). The yield surface in ABAQUS is defined by four constitutive parameters: the ratio of the second stress invariant on the tensile to compressive meridian (K_c), Poisson's ratio, eccentricity (ϵ), angle of dilation (ψ), and biaxial to uniaxial compressive yield stress ratio (σ_{b0}/σ_{c0}). Below the critical stress threshold, where concrete displays enhanced plastic volume, Poisson's ratio regulates volume fluctuations. This is measured at high confining pressure by the angle of dilation (ψ), which is found by sensitivity analysis. The value of eccentricity (ρ) is 0.1 by default. Based on complete triaxial tests of concrete, K_c , usually 2 or 3, is defined. The default value of the ratio σ_{b0}/σ_{c0} is 1.16. (Manual for Abaqus, 2008). This study uses default values for ϵ , σ_{b0}/σ_{c0} , and K_c due to the lack of specific test data.

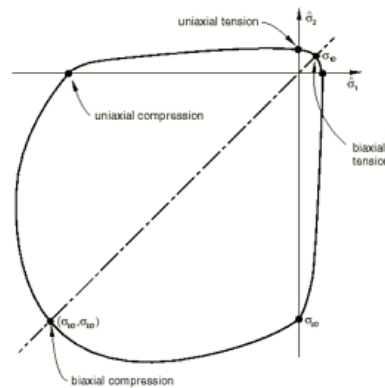


Figure 3: Biaxial yield surface in CDP Model (Abaqus User Manual, 2000)

The behavior of concrete has been simulated using a constitutive model of concrete damage. The concrete's response is approximated using CDP when the main stress components are primarily compressive.

Table 1: Material Properties for Circular Steel-Concrete Composite Column (CDP Model for Concrete Class B50)

Circular steel concrete composite column		CDP model for concrete class B50				
Young's Modulus (E_a)	Poisson's Ratio (ν_c)	Dilation Angle	Eccentricity	f_{b0}/f_{c0}	k	Viscosity Parameter
38500 MPa	0.3	38	0.1	1.12	.666	0

Table 2: Mechanical Properties of Concrete

Compressive Behavior concrete		Tensile Behavior of concrete	
Yield Stress	Inelastic Strain	Yield Stress	Cracking Strain
15	0	1.99893	0
20.197804	7.47307E-005	2.842	3.333E-005
30.000609	9.88479E-005	1.86981	0.000160427
40.303781	0.000154123	0.862723	0.000279763
50.007692	0.000761538	0.226254	0.000684593
40.23609	0.002557559	0.056576	0.00108673
20.23609	0.005675431		
5.257557	0.011733119		

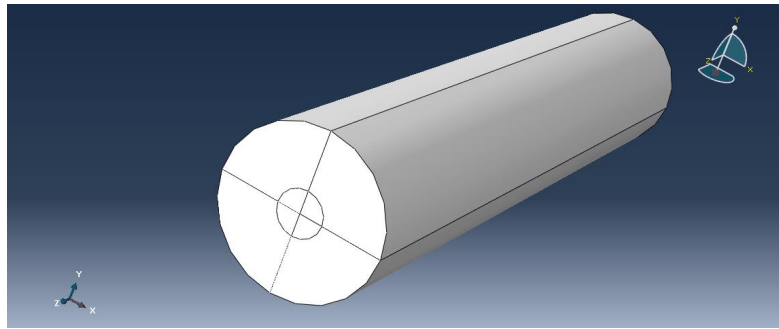


Figure 4: Concrete column model on ABAQUS

In this model, elastoplastic steel was utilized to create composite members that combine the advantages of both concrete and elasto-plastic steel. The whole stress-strain relationship obtained from uniaxial tension testing performed on specimens removed from the steel tubes was used for the FE studies.

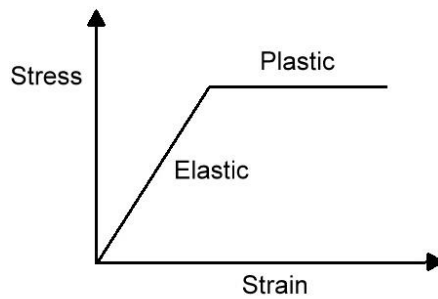


Figure 5: Stress vs. Strain Curve of Elasto-plastic steel

Table 3: Properties of steel

Young’s Modulus	Poisson’s Ratio	Yield Stress	Plastic strain
206000	0.3	433	0

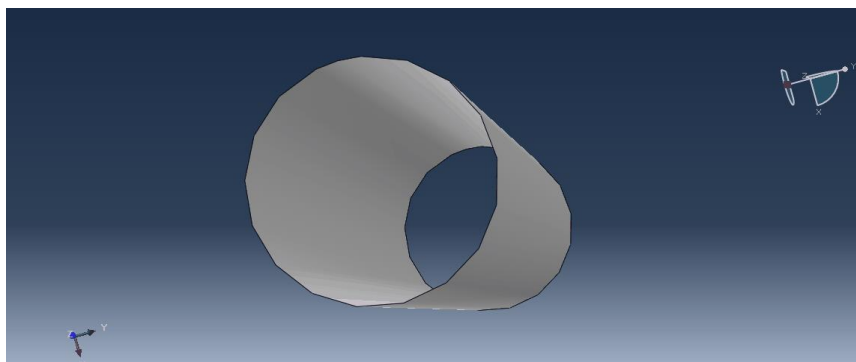


Figure 6: Steel tube model on ABAQUS

2.1 Models generated for 3 different cases

This table represents three different cases of CFT column and the shell thickness and height of the column. There are different diameters (160 mm, 150 mm, and 140 mm) are used for the purpose of parametric study. In case 2, the diameter and height were fixed for CFT column but the shell thickness

was varied with 6 mm, 4 mm and 3 mm. At last, in case 3, the height of the column was changed with 600 mm, 500 mm and 400 mm and diameter and the shell thickness were fixed at that time.

Table 4: Dimensions of CFT column in different models

Case	Model	Diameter (mm)	Shell thickness (mm)	Height (mm)
1	1	160	4.8	650
	2	150	4.8	650
	3	140	4.8	650
2	4	157	6	650
	5	157	4	650
	6	157	3	650
3	7	157	4.8	600
	8	157 <td 4.8	500	
	9	157	4.8	400

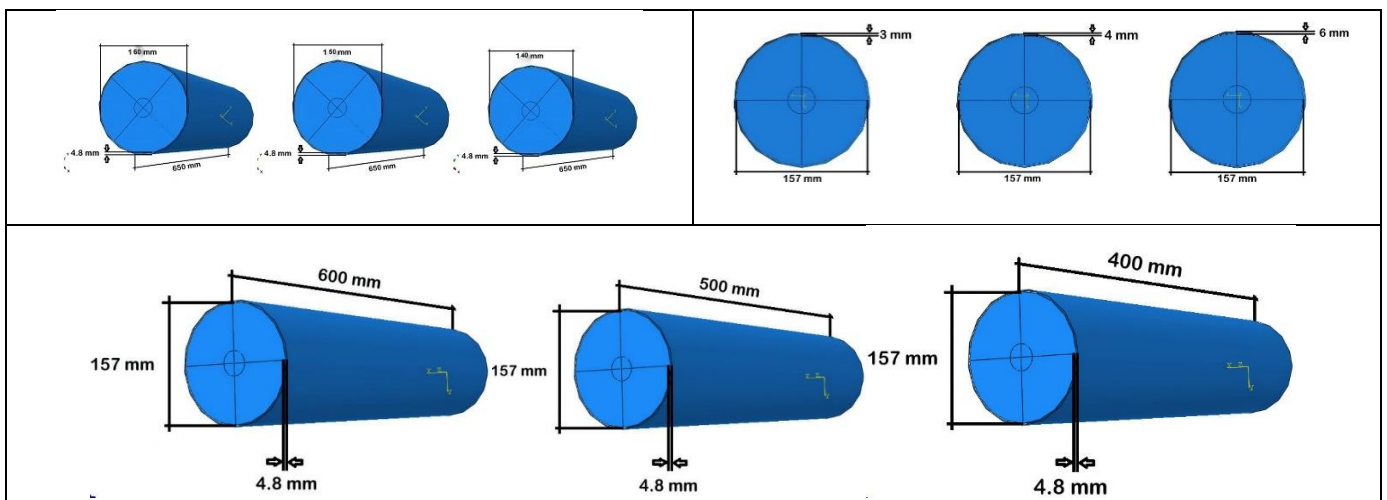


Figure 7: 3D dimension of CFT column

The manual meshing was used for both concrete and steel to achieve a better model response for advanced results. A surface-based interaction with tie constraints was utilized to model the connection with the tube of steel and the concrete core. The concentrated load will get divided into number of nodes in node set equally. Load was applied at “surf 1” and opposite surface ‘surf 2’ is supported as fixed support as shown in the figure 08.



Figure 8: Load in one end of the model

3. Result and Discussion

3.1 Analysis of model with different diameters

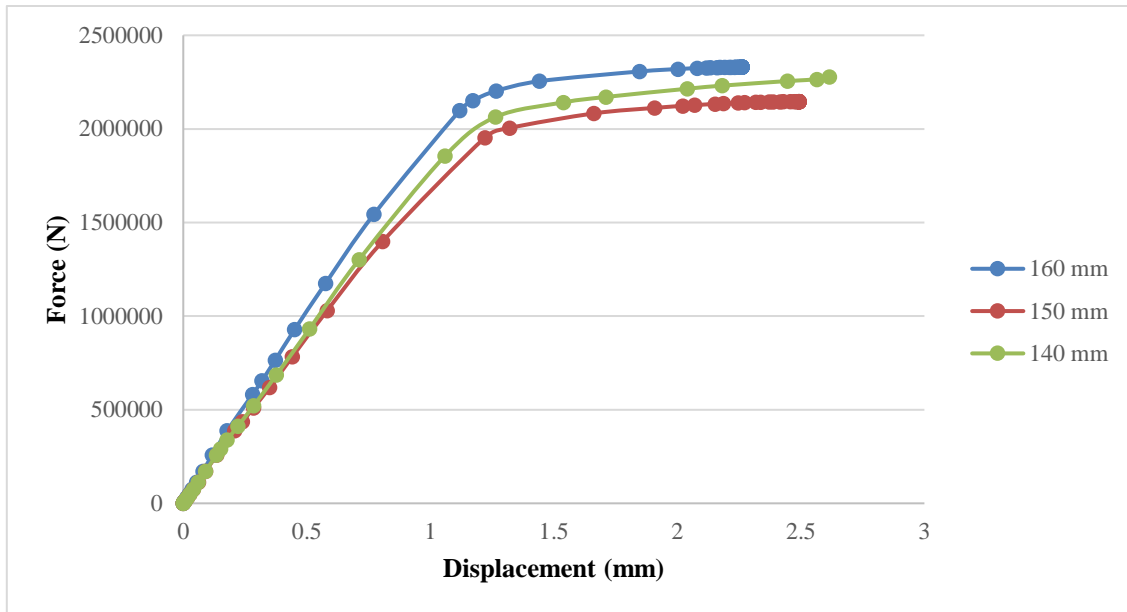


Figure 9: Force vs. displacement curve for different diameter of concrete tube

Figure 9 illustrate that the three different diameters of tubes, three distinct forces vs. displacement curves were obtained. Model 1, with a diameter of 160 mm, exhibits the lowest displacement value of approximately 2.26 mm and a capacity of nearly 2330 kN. In comparison, Model 2 and Model 3, with diameters of 150 mm and 140 mm respectively, show higher displacements of 2.49 mm and 2.61 mm. For a hollow tube with a diameter of 157 mm, the capacity was found to be 2150 kN. When comparing the deviations in capacity between the 157 mm tube and the other models, it observes an 8.37% deviation for the 160 mm model, a 1.41% deviation for the 150 mm model, and a 6.97% deviation for the 140 mm model. This indicates that as the column diameter increases, the displacement decreases.

3.2 Analysis of model with different shell thickness of hollow tube

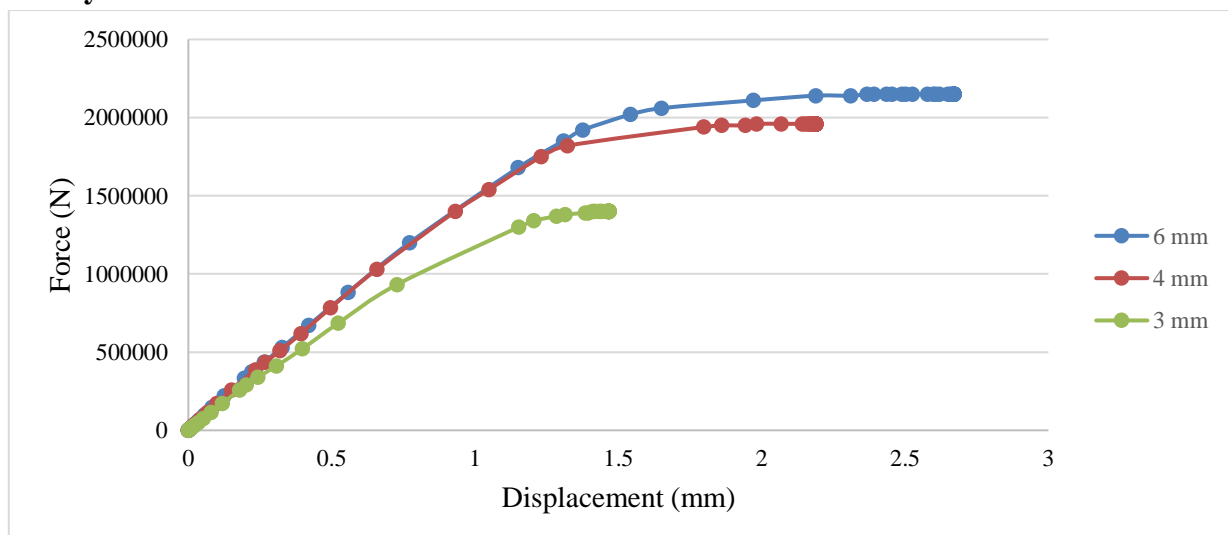


Figure 10: Force vs. displacement curve for different shell thickness of hollow tube

Figure 10 describe that the three different shell thicknesses of a hollow tube, three distinct forces vs. displacement curves were obtained. Model 1 has a shell thickness of 6 mm, while Models 2 and 3 have shell thicknesses of 4 mm and 3 mm, respectively. According to the diagram, Model 1 shows the highest displacement value, approximately 2.67 mm, and a force of nearly 2170 kN. Model 2 has a displacement value of 2.18 mm and a capacity of 1960 kN. Model 3, with the lowest displacement value of 1.46 mm, has a capacity of 1400 kN. When the thickness increased from 4.8 mm to 6 mm, the capacity deviation was 0.93%. A decrease in thickness from 4.8 mm to 4 mm resulted in a deviation of 8.83%, and a decrease from 4.8 mm to 3 mm led to a deviation of 34.88%. This indicates that as the thickness decreases, the deviation in capacity increases.

3.3 Analysis of model with different slenderness ratio

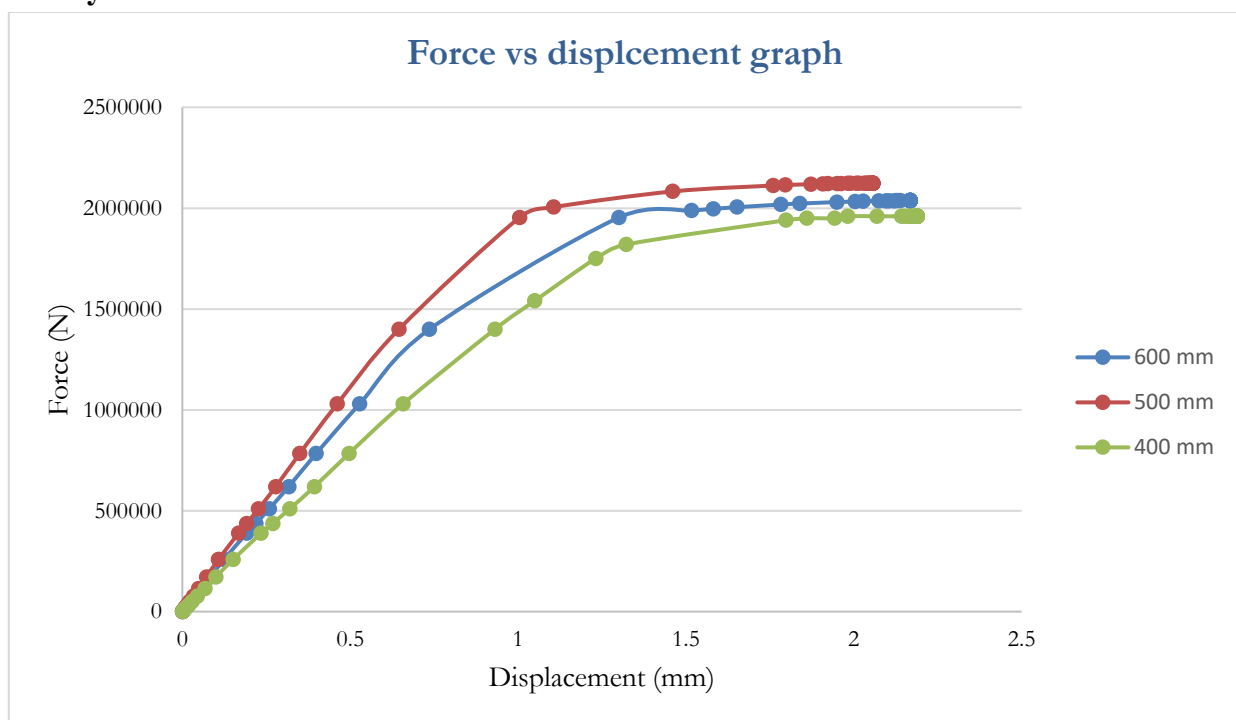


Figure 11: Force vs. displacement curve for different slenderness ratio of tube

Figure 11 demonstrate that the three different slenderness ratios of hollow tube shell thicknesses, three distinct forces vs. displacement curves were obtained, using models with three different heights. According to the diagram, Model 1 has the highest displacement value, nearly 2.05 mm, and a capacity of 2120 kN. Models 2 and 3 exhibit relatively lower force and displacement values. When comparing the deviation in capacity between the models with heights of 650 mm and 600 mm, the deviation is 1.39%. The deviation between the 650 mm and 500 mm models is 5.11%, and between the 650 mm and 400 mm models, it is 8.83%. This indicates that as the height of the column decreases, the deviation in capacity increases.

4. Conclusion:

A numerical analysis of CFT stub columns under conditions of concentrically loaded conditions is presented in this work. The influence of several characteristics, such as concrete strength, load carrying

capacity of the column, and deformation measurement techniques, was examined based on specimen behavior observations.

- Load carrying capacity of CFT column was observed in different conditions i.e. changing diameter, changing shell thickness and different slenderness ratio.
- Results were validated with test results of the entire section of CFT column only. The experiment can be carried out for concrete section, Steel section and empty steel tube also.
- Concrete damaged plasticity model was used for non-linear analysis.
- Change of displacement and percentage of errors occurred due to analysis with different variables.
- Parametric studies done with different diameters showed that the displacement decreases with the increase of column diameter. For diameters of 160mm, 150mm & 140mm capacity deviates 8.37%, 1.41% & 6.97% respectively from test result.
- Parametric studies done with different shell thickness showed that capacity increases with increase in shell thickness. For shell thickness of 6mm, 4mm & 2mm capacity deviates 0.93%, 8.83% & 34.88% respectively from test result.
- It was also noticed that the capacity of column increases with the increase in column height. For height of 600mm, 500mm & 400mm capacity deviates 1.39%, 5.11% & 8.83% respectively from test result.

5. References

1. Claeson, C. (1998). "Structural behavior of reinforced high-strength concrete columns." PhD thesis, Div. of Concrete Struct., Chalmers Univ. of Technology, Gothenburg, Sweden.
2. Johansson, M. and Gylltoft, K. (2002) 'Mechanical behavior of circular steel-concrete composite stub columns', *Journal of Structural Engineering*, 128(8), pp. 1073–1081. doi:10.1061/(asce)0733-9445(2002)128:8(1073).
3. Huang, C.S. et al. (2002) 'Axial load behavior of stiffened concrete-filled steel columns', *Journal of Structural Engineering*, 128(9), pp. 1222–1230. doi:10.1061/(asce)0733-9445(2002)128:9(1222).
4. Sakino, K. et al. (2004) 'Behavior of centrally loaded concrete-filled steel-tube short columns', *Journal of Structural Engineering*, 130(2), pp. 180–188. doi:10.1061/(asce)0733-9445(2004)130:2(180).
5. Giakoumelis, G. and Lam, D. (2004) 'Axial capacity of circular concrete-filled tube columns', *Journal of Constructional Steel Research*, 60(7), pp. 1049–1068. doi:10.1016/j.jcsr.2003.10.001.
6. Hu, H.-T. et al. (2003) 'Nonlinear analysis of axially loaded concrete-filled tube columns with confinement effect', *Journal of Structural Engineering*, 129(10), pp. 1322–1329. doi:10.1061/(asce)0733-9445(2003)129:10(1322).
7. Ellobody, E., Young, B. and Lam, D. (2006) 'Behaviour of normal and high strength concrete-filled compact steel tube circular stub columns', *Journal of Constructional Steel Research*, 62(7), pp. 706–715. doi:10.1016/j.jcsr.2005.11.002.
8. Campian, C., Nagy, Z. and Pop, M. (2015) 'Behavior of fully encased steel-concrete composite columns subjected to monotonic and cyclic loading', *Procedia Engineering*, 117, pp. 439–451. doi:10.1016/j.proeng.2015.08.193.
9. Liang, Q.Q. and Fragomeni, S. (2009) 'Nonlinear analysis of circular concrete-filled steel tubular short columns under axial loading', *Journal of Constructional Steel Research*, 65(12), pp. 2186–2196. doi:10.1016/j.jcsr.2009.06.015.

10. Tomii M, Yoshimura K, Morishita Y. Experimental studies on concrete filled steel tubular stub columns under concentric loading. In: Proceedings of the international colloquium on stability of structures under static and dynamic loads. 1977. p. 718–41.
11. SSALEH, S.M. and AL-ABBOODĪ, Ī. (2021) ‘Strength and behaviour assessment of axially loaded concrete filled steel tubular stub columns’, Turkish Journal of Engineering, 5(4), pp. 154–164. doi:10.31127/tuje.686246.
12. Zeghiche, J. and Chaoui, K. (2005) ‘An experimental behaviour of concrete-filled steel tubular columns’, Journal of Constructional Steel Research, 61(1), pp. 53–66. doi:10.1016/j.jcsr.2004.06.006.
13. Tomasz Jankowiak, Tomasz Lodygowski, Identification of Parameters of Concrete Damage Plasticity Constitutive Model (2005), ISSN 1642-9303.
14. The ABAQUS User Manual (2008).